Sensation seeking correlates with increased white and grey matter integrity of structures associated with visuospatial and decision-making processing in healthy adults

Andrea Escelsior (andrea.escelsior@live.com)
IRCCS Ospedale Policlinico San Martino
Alberto Inuggi
University of Genoa
Maria Bianca Amadeo
U-VIP Unit for Visually Impaired People, Fondazione Istituto Italiano di Tecnologia
Batya Engel-Yeger
University of Haifa
Alice Trabucco
IRCCS Ospedale Policlinico San Martino
Davide Esposito
U-VIP Unit for Visually Impaired People, Fondazione Istituto Italiano di Tecnologia
Claudio Campus
U-VIP Unit for Visually Impaired People, Fondazione Istituto Italiano di Tecnologia
Beatriz Pereira
University of Genoa
Gianluca Serafini
IRCCS Ospedale Policlinico San Martino
Monica Gori
U-VIP Unit for Visually Impaired People, Fondazione Istituto Italiano di Tecnologia
Mario Amore
IRCCS Ospedale Policlinico San Martino

Article

Keywords: Sensory Profile, Healthy Adults, Neuroimaging, Sensation Seeking, Visuospatial Processing, Affective Regulation

Posted Date: July 12th, 2022

DOI: https://doi.org/10.21203/rs.3.rs-1797604/v1

Abstract

Background: The ability to process sensory information is an essential adaptive function, and hyper- or hypo-sensitive maladaptive profiles of repones to environmental stimuli generate sensory processing disorders linked to cognitive, affective, and behavioural alterations. The research on neuroradiological correlates of the sensory processing profiles is still in its infancy and is mainly limited to the young-age population or neurodevelopmental disorders. So, the knowledge concerning the impact of the different sensory profiles on the structural and functional characteristics of the typically developed adult brain remains largely obscure. In this framework, this study aims to examine the structural and functional MRI correlates of sensory profiles in a sample of healthy adults.

Method: We investigated structural T1, Diffusion Tensor Imaging (DTI), and resting-state functional MRI (rs-fMRI) correlates of Adolescent/Adult Sensory Profile (AASP) questionnaire subscales in 57 typical developing subjects (34 females; mean age: 32.7±9.3).

Results: Only the AASP sensation seeking subscale provided significant results. Positive and negative correlations emerged with FA and RD in arcuate fasciculus (AF), anterior thalamic radiation (ATR), optic radiation (OR), superior longitudinal fasciculus (SLF), corpus callosum (CC), and the dorsal part of the cingulum bundle (dCB). In addition, we found a positive correlation between sensation seeking and grey matter volume in the parahippocampal cortex (PHC), precentral gyrus (PG), inferior temporal gyrus (IFG) and cuneus regions, and with cortical thickness in the IFG and postcentral gyrus (PCG). We did not find any correlation between rs-fMRI parameters and AASP subscales.

Conclusion: Overall, our results suggest a positive correlation between sensation seeking and higher structural integrity in critical regions mainly involved in visuospatial and decision-making processing. We speculate that the better structural integrity associated with sensation seeking might at least partially reflect a possible neurobiological substrate of this sensory profile, characterized by active research of sensory stimuli and impulsive decision-making tendency. Further studies are needed to investigate the neuroradiological correlates of sensory profiles and their impact on behaviour, cognition, and affectivity in different developmental stages and psychiatric disorders.

Introduction

Sensory processing. Sensory processing is a process that requires gathering and interpreting exogenous and endogenous sensory information (e.g., taste, touch, smell, sight, hearing, equilibrium, pain). It is fundamental for life, it constantly drives interactions between an organism and its environment, allowing an adaptive response to ambient changes [1]. Sensory processing alterations, expressed in hypo or hypersensitivity, profoundly affect daily functioning. The functional impact of these alterations defined the Sensory Processing Disorders (SPD) condition. Given the importance of sensory processing, it is not surprising that SPD is associated with sensory, cognitive, and emotional alterations. Thus, it may lead to behavioural alterations and be related to different mental disorders [2–4], their clinical severity, and burden

of comorbidity [4–6]. Despite the crucial importance of sensory processing in shaping normal and psychopathological behaviours, this topic is almost exclusively investigated by occupational therapists [7]. Moreover, the available knowledge regarding the neuroradiological correlates of sensory profiles is limited to a few articles, mainly focused on young-aged, typically developed populations [8,9] and neurodevelopmental disorders [10,11].

The Dunn's model of sensory processing. Dunn's model provides a conceptual framework to interpret individual-specific behaviours as responses to different sensory processing patterns [12]. The model describes the interaction between the neurological threshold to sensory stimuli (low or high) and the individual's behavioural strategy to deal with their neurological threshold, i.e., active or passive. The behavioural response continuum indicates the ability to respond according to one's neurological threshold. The model distinguishes four different profiles: low registration, sensation seeking, sensory sensitivity and sensation avoidance [12]. Specifically, *low registration* subjects have a reduced ability to perceive sensory stimuli due to a higher neurological threshold and a passive strategy, meaning that they do not actively seek rich sensory input that reaches their threshold. As opposed to that, *sensation seekers* have a higher neurological threshold and active behavioural self-regulation strategies. They actively search for intense stimuli like places with bright lights, colours, and sounds (as in parties and malls). Sensation seekers are often characterized by a tendency to impulsive decision-making processes [13]. Furthermore, this profile is associated with increased motor behaviours [14], attachment security [15], extroversion and reduced interpersonal boundaries [16]. Subjects with *sensory sensitivity* have a low neurological threshold and a passive strategy, meaning they do not actively limit their exposure to unpleasant sensory stimuli. *Sensation-avoiding* subjects have a low neurological threshold and active behavioural self-regulation strategies, they avoid overwhelming sensory input and follow routine habits [12].

Current findings on the neurobiological substrates of sensory profiles. In recent years researchers have addressed the topic of the neurobiological underpinnings of sensory profiles. In the healthy population, to our knowledge, only one study explored the correlations between white matter (WM) alterations and sensory processing using the Adolescent/Adult Sensory Profile (AASP) questionnaire [8]. They reported a positive correlation between the Diffusion Tensor Imaging (DTI) microstructural alterations of the right uncinate and cingulate tracts and the sensory sensitivity scores in a sample of 84 healthy young adults (42 females) aged 24.5±4.7 (range: 19–39 years) [8]. As observed by the authors, their results *"should not be applied to other developmental stages",* and they highlight the *need for "more studies involving participants in other development stages"* in consideration of the young age of their sample and the maturational changes of the white matter during normal development. Yoshimura and colleagues examined the differences in grey matter (GM) volume related to sensory profiles in 51 young, healthy volunteers (26 females) aged: 22.5±4.5 (range: 19-43 years). They reported a positive correlation between sensory sensitivity scores and the left dorsolateral PFC volume [9]. Among clinical populations, neuroimaging studies on sensory profiles consist of case-control studies on neurodevelopmental

disorders. For example, Owen et al. reported among children with SPD a decreased fractional anisotropy (FA) and increased mean diffusivity (MD) and radial diffusivity (RD), particularly in the posterior CC corona radiata and thalamic radiations [11]. In a recent study, adults with autism spectrum disorder (ASD) and attention deficit hyperactivity disorder (ADHD) displayed a correlation between sensory sensitivity scores and RD in the posterior CC [10]. However, further research is needed to find objective measures that provide possible explanations for neural mechanisms underlying the linkage between sensory processing and psychopathology [17].

Aim of the study

Available literature reported the need to fill the lack of knowledge regarding the neuroradiological correlates of sensory profiles in healthy adults. So, we aimed to examine the MRI correlates of sensory profiles in a sample of typically developed adult individuals with different techniques: structural T1, DTI and resting-state functional MRI (rs-fMRI).

Results

Sociodemographic characteristics. Thirty-four females and twenty-three males (mean age±standard deviation (SD) = 32.7±9.3 years), typically developing right-handed subjects, participated in this study. **Table 1** depicts the sociodemographic characteristics of the sample as measured by the ranges, mean, and SD scores.

Questionnaires analysis. Table 1 depicts the number and per cent of subjects with scores under the norm, in the normal range, and above the norm for each sensory profile. We did not find significant age and gender differences in mean AASP subscale scores (see **Supplementary materials**).

Table 1. Sociodemographic characteristics and sensory profiles quadrant scores distribution of the sample

Variable	Mean	SD	Range	
Number (N)	57			
Age	32.7	9.3	20-59	
Gender, female (male)	34 (23)			
Race, Caucasian	57			
Dominant hand (right)	57			
BMI Kg/m^2	23.2	2.1	17.8-27.7	
Full scale IQ	102	13	87-132	
Sensory Profile		**N**	**%**	**Range**
Low registration	Under norm	15	26.3	15-23
	Norm	32	56.1	24-35
	Above norm	10	17.5	36-75
Sensation Seeking	Under norm	19	33.3	15-42
	Norm	35	61.4	43-56
	Above norm	3	5.3	57-75
Sensory sensitivity	Under norm	10	17.5	15-25
	Norm	36	63.2	26-41
	Above norm	11	19.3	42-75
Sensation Avoiding	Under norm	6	10.5	15-26
	Norm	40	70.2	27-41
	Above norm	11	19.3	42-75

TBSS analysis. Analysis of MD and AD did not reveal any significant correlation with any sensory profile. FA and RD were found instead, respectively positively and negatively correlated to the sensation seeking profile in a total of 9408 and 12443 voxels. Results are displayed in **Figure 1**.

Segmentation of TBSS results with XTRACT atlas. We segmented both FA and radD significant TBSS maps with each XTRACT tract's skeletonized version and found that 15 and 17 tracts had a fraction (higher than 10%) of their voxels' values, respectively FA and RD, correlated with the SP_STS score. The coverage percentages within each of these tracts are summarized in **Table 2.**

Pearson correlation analysis confirmed their correlation with *sensation seeking* (columns tbss-R and tbss-P of **Table 2**). Through the automated xTract tractography analysis, we reconstructed these tracts (CC is

not present in the XTRACT atlas) in each subject's native space, we calculated their mean FA and radD and correlated it with SP_STS, results are summarized in columns xTract-R and xTract-P of **Table 2**.

Table 2. Correlations between sensation seeking and DTI metrics: FA (left) and RD (right) of whole-brain TBSS and xTract based analyses. cov %: percentage of voxels within each xTract tract that TBSS analysis found significantly correlated with sensation seeking. Correlation between sensation seeking and significant voxels of TBSS (tbss-R and tbss-P). Correlation between sensation seeking and all voxels of each XTRACT's tract (Xtract-R and Xtract-P). R= regression coefficient, p=statistical significance, n.s.= not significant.

	FA					RD				
	TBSS			xTract		TBSS			xTract	
tract	cov %	R	P	R	p	cov %	R	p	R	p
af_r	13.1	0.51	<.0001	0.23	0.093	12.9	-0.37	0.0041	-0.23	0.1
atr_l	12.2	0.5	<.0001	0.31	0.021	17.6	-0.49	<.0001	-0.36	0.008
atr_r	13.3	0.54	<.0001	0.3	0.029	13.7	-0.5	<.0001	-0.36	0.007
cbd_l	25.7	0.45	<.001	0.41	0.0018	22.4	-0.45	<.001	-0.33	0.016
cbp_l	45.0	0.3	0.024	n.s.	n.s.	11.4	-0.31	0.017	n.s.	n.s
cst_r	–	–	–	–	–	11.3	-0.46	<.001	-0.34	0.012
fa_l	10.1	0.38	0.0035	0.28	0.042	12.4	-0.42	0.0011	n.s.	n.s.
fa_r	10.8	0.43	<.001	0.28	0.041	12.4	-0.45	<.001	n.s.	n.s.
fmi	27.4	0.49	<.0001	0.29	0.036	43.1	-0.47	<.001	n.s.	n.s.
mdlf_r	10.5	0.47	<.001	0.34	0.013	10.7	-0.46	<.001	-0.35	0.008
or_r	14	0.38	0.0033	0.37	0.0066	13.7	-0.41	0.0016	-0.28	0.04
slf1_l	13.1	0.44	<.001	0.33	0.013	18.3	-0.42	0.001	-0.31	0.025
slf1_r	15.6	0.5	<.0001	0.3	0.025	28.7	-0.43	<.001	n.s.	n.s.
slf2_r	24.3	0.56	<.0001	0.35	0.01	24.3	-0.46	<.001	-0.34	0.012
slf3_r	12.6	0.53	<.0001	n.s	n.s	–	–	–	–	–
cc	19.9	0.55	<.0001	0.41	0.003	27	-0.52	<.0001	-0.38	0.011
uf_l	–	–	–	–	–	15.2	-0.4	0.0021	-0.26	0.011
str_r	–	–	–	–	–	10.4	-0.4	0.0019	-0.25	0.013

Abbreviations: af, Arcuate Fasciculus, **atr**, Anterior Thalamic Radiation, **cc**, Corpus Callosum, **cbd**, Cingulum subsection: Dorsal, **cbp** Cingulum subsection: Peri-genual, **cst**, Corticospinal Tract, **fa**, Frontal Aslant Tract, **fmi**, Forceps Minor, **l**, left, **mdlf**, Middle Longitudinal Fasciculus, **or**, Optic Radiation, **r**, right, **slf**, Superior Longitudinal Fasciculus, **str**, Superior Thalamic Radiation, **uf**, Uncinate Fasciculus.

Other whole-brain analysis. Whole-brain VBM and CT analysis did not reveal any significant voxel/vertices correlated to any sensory profile dimension. After dual-regression analysis, the same occurred analyzing within-network connectivity (see supplementary materials).

Second stage analysis. We thus focused our attention on the *sensation seeking* profile, looking for its correlation with ROI-based structural metrics. In none of the ROIs of Neuromorphmetric atlas, the WM volumes correlated with it. Instead, its GM volumes did it positively in the left and right parahippocampal cortex (PHC), the right precentral (PG), and inferior temporal (ITG) gyri, and cuneus. Values are summarized in **Table 3** and displayed in **Figure 2**. CT mean values within the a2000s atlas positively correlated with *sensation seeking* profiles in the right and left postcentral (PCG) and left inferior frontal (IFG) gyri. Values are summarized in **Table 3** and displayed in **Figure 3**.

Table 3. Correlations between sensation seeking and gray matter volumes (left) and cortical thickness (right) in five and three ROIs, respectively, belonging to the Neuromorphmetrics and a2000s atlases. R= regression coefficient, p=statistical significance.

GM VOLUMES	R	p	CT	R	p
L PHC	0.35	0.008	L IFG	0.33	0.014
R PHC	0.41	0.0018	L Postcentral gyrus	0.32	0.016
R Precentral gyrus	0.32	0.017	R Postcentral gyrus	0.38	0.004
R ITG	0.35	0.0079			
R Cuneal cortex	0.3	0.023			

Abbreviations: IFG, inferior frontal gyrus**, ITG,** inferior temporal gyrus**, L,** left**, PHC,** parahippocampal cortex**, R,** right

rs-fMRI analyses. The rs-fMRI analyses did not show any significant correlation between any resting-state network and any AASP subscale. Details are summarized in **Supplementary Materials**.

Discussion

To the best of our knowledge, this is the first study evaluating sensory processing patterns using different structural and functional MRI measures in healthy adults. The study's preliminary results showed a strong correlation between the AASP sensation seeking subscale score and several WM tracts involved in visuospatial sensory processing and affective regulation. More precisely, we found a positive and a

negative correlation with both FA and RD in arcuate fasciculus (AF), anterior thalamic radiation (ATR), optic radiation (OR), superior longitudinal fasciculus (SLF), corpus callosum (CC), and the dorsal part of the cingulum bundle (dCB). We did not find significant correlations between AASP dimensions, whole-brain structural data (VBM and CT), or within-network FC indices. When we explored the partial correlation between sensation seeking and structural metrics within the ROIs of a well-known atlas, we found positive correlations in both GM volumes and CT in a few of those ROIs.

Tracts with enhanced white matter integrity among sensation seekers. As previously reported, our results highlight the correlation between better integrity of the WM in multisensory and affective brain regions with sensation seeking scores.

The optic radiation. The OR is a tract implicated in low-level simple visual processing [29], conveying visual inputs mainly from the magnocellular and parvocellular pathways, which project the visual dorsal and the ventral streams [30].

The superior longitudinal and the arcuate fasciculi. The SLF and the AF are distinct WM tracts with different functions [31]. The SFL includes mainly frontoparietal and, to a lesser extent, frontotemporal connections [32]. Anatomically, the SLF comprises three subcomponents (SLF I, II, and III) [31]. AF, SLF II, and SLF III are involved in auditory processing in the dominant hemisphere and visuospatial processing in the right hemisphere [33], moreover, AF and SLF III are implicated in facial emotion recognition [34]. These WM connections mainly belong to the frontoparietal network and are crucial for sensory processing, cognitive functions, metacognition and empathy [32].

The anterior thalamic radiation. The ATR fibers mainly connect the mediodorsal thalamic nuclei with the PFC [35], the anterior thalamic nuclei and the anterior cingulate cortices [36]. The ATR mediate complex behaviour planning [37] and affective regulation [38]. Interestingly, children with SPD displayed cognitive and visuomotor control impairments linked to reduced FA in ATR and SLF [39]. In children, sensation seeking, assessed through the UPPS-P scale, results negatively associated with sensation seeking [40].

The corpus callosum. The CC plays an essential role in the communication between the hemispheres [41], allowing the multidimensional representation of information and adaptative coordination of sensorimotor, affective and cognitive functions [42]. The CC displays high plasticity in response to environmental stimuli [41,43], and its structural integrity is associated with stress resilience [44], whereas reduced integrity is common among mental illnesses.

The dorsal tract of the cingulum bundle. The CB is a vast WM structure connecting subcortical regions to the cingulate cortex and connecting parietal and medial temporal cortices [45]. The cingulum is a highly environment-sensitive structure with a prolonged development. This reason might explain its crucial role in affective and neurocognitive differences between subjects [46] and its essential role in psychopathology [45]. Interestingly, the dorsal cingulate region is crucially involved in emotional self-control and dopamine-

mediated reward prediction, providing adaptive decision-making responses to environmental conditions [47,48] and higher cognitive control [49].

Differences in grey matter volume and cortical thickness in sensation seekers. A correlation was found between sensation seeking scores and an increased GM volume in the PHC, PG, ITG, and cuneus. The PHC comprises a vast part of the medial temporal lobe and plays an essential role in visuospatial processing and episodic memory [50]. The PG is the site of the primary motor cortex, which subserves motor functions and multisensory integration [51]. The ITG has different functions. As part of the ventral visual pathway, it is involved in the visual processing of colours, faces, and shapes [52], moreover, it regulates emotion, language, and decision making [53]. The cuneus covers part of the occipital lobe and facilitates the functioning of the dorsal and ventral visual streams, thus allowing basic and higher-order visual processing [54]. Our results resemble those previously reported by Chen and colleagues in a large study (n=11474) on the adolescent brain, sensation seeking dimension, measured through the UPPS-P scale, is associated with volumetric alteration, with increased grey matter volume in several regions, including parietal, temporal, frontal, hippocampal and cingulate cortices [55].

Regarding CT, a positive correlation was found between sensation seeking scores and IFG and PCG. The IFG is part of the prefrontal cortex (PFC) [56]. The left IGF is functionally involved in language processing [57], inhibitory control [58,59], perception, imitation and internal representation of movements, and working memory [60,61]. The PCG corresponds to the primary somatosensory cortex [62], which is crucially involved in multisensory integration [63,64].

Functional connectivity in sensation seekers individuals. Following the classical approach, when strong a-priori hypotheses are missing, we started to explore the within-network FC of the DMN, the main functional brain hub at rest. According to existing literature that associated the sensation seeking profile with increased motor behaviours [14] and describes these individuals as constantly researching environmental inputs [12], within-network connectivity was also run in sensorimotor, primarily visual, lateral occipital and auditory-related RSNs. According to the present results, none of the AASP subscales had a relationship with FC at rest.

Conclusions

Here, we reported that a tendency to sensation seeking in healthy subjects is strongly associated with a higher white matter and grey matter structural integrity in areas mainly involved in visuospatial processing and decision-making functions. Notably, the sensation seeking profile is usually associated with a tendency to actively pursue novel sensory experiences and a tendency to impulsive decision-making processes. In this framework, we speculate that the better structural integrity associated with

sensation seeking might reflect, at least in part, a possible neurobiological substrate of this sensory profile.

Methods

Participants and procedure. Inclusion criteria are 1) age greater than 18 years, 2) willingness to participate in the study, 3) normal range for full-scale intelligence quotient scores measured with the Wechsler Adult Intelligence Scale, Third Edition, and 3) spoken language: Italian. Exclusion criteria are 1) history of psychiatric disorders, assessed through the Italian version of the Mini-International Neuropsychiatric Interview [18], 2) first-degree familiarity with neuropsychiatric disorders, 3) presence of severe neurological and medical illnesses (e.g., vascular diseases, cancer), 4) alcohol and substance abuse during the previous three months and 5) the inability to undergo an MRI examination. In addition, sociodemographic data and medical and psychiatric status information were collected.

Furthermore, each participant responds to the AASP, a 60-items self-report questionnaire used to assess sensory processing patterns [8]. The items are sorted equally into four traits reflecting Dunn's model. The questionnaire requests the participants to indicate the frequency of their behavioural responses to sensory experiences in daily life on a five-point Likert scale. Norms exist for different age groups.

Ethics approval. The study was granted the approval of the the Ethical Committee of IRCCS Ospedale Policlinico San Martino, and all subjects gave informed consent. The study was performed in accordance with the relevant ethical guidelines and regulations

Statistical analysis. Statistical analysis was performed using R software.

MRI data

MRI recording. A 1.5-T GE scanner with a standard head coil was used. Foam pads were used to reduce head motion and scanner noise. Three-dimensional T1-weighted anatomical images were acquired in a sagittal orientation employing a 3D-SPGR sequence (TR/TE=11.5/5 ms, IR=500 ms, flip angle=8 degree, FOV=25.6 cm) with a resolution in-plane of 256x256 and slice thickness of 1 mm. DTI was acquired with a pure axial single-shot echo-planar imaging sequence. The diffusion sensitizing gradients were applied along 60 non-collinear directions (b=1000 s/mm^2), together with 5 acquisitions without diffusion weighting (b=0). Fifty-five contiguous axial slices were acquired with a slice thickness of 2.5 mm without a gap. The acquisition parameters were as follows: TR/TE=13750/93 ms, image matrix=128x128, FOV=24 cm, NEX=1. fMRI scanning was carried out in the dark, with participants instructed to keep their eyes closed, relax, and move as little as possible. Functional images were collected using a gradient Echo Planar Imaging (EPI) sequence sensitive to Blood-Oxygen-Level Dependent (BOLD) contrast (TR/TE = 2000/30 ms, flip angle = 90°, FOV = 24 cm). Whole-brain volumes were acquired in 33 contiguous 4-mm-thick transverse slices, with a 1-mm gap and 3.75 × 3.75-mm^2 in-plane resolution. For each participant, fMRI scanning lasted 5 min and acquired 150 scans.

MRI processing. This study aimed to correlate the four sensory profiles to all the MRI sequences we recorded. In a first stage analysis, we run correlation analysis with anatomical, resting state, and diffusion data at the whole-brain level. From anatomical data, we investigated CT and voxel-based morphometry. We run a within-network melodic analysis from EPI recording at rest and an FSLNets one. We run a preliminary TBSS analysis from diffusion data to define which tract reconstruct with tractography and then calculate their mean metrics. In a second stage analysis, since we found that only the sensation seeking profile correlated with our whole brain data (specifically DTI one), we ran a correlation analysis between such sensory dimension and ROI-based structural values. Since we did not find any results related to resting-state data, its detailed processing methods were described only in supplementary materials.

Anatomical data. 3D T1-weighted MRI scans were converted to NIFTI format and resliced from sagittal to axial orientation. They were visually inspected, and their origin was set in correspondence with the anterior commissure. The following processes were then carried out with the Computational Analysis Toolbox (CAT, version 12.6) within SPM12 using MATLAB (version 2017b). All images were normalized using an affine followed by non-linear registration, corrected for bias field inhomogeneity, and then segmented into GM, WM, and CSF components [19]. Using six iterations, the Diffeomorphic Anatomic Registration Through Exponentiated Lie (DARTEL) algebra algorithm normalizes the segmented scans into a standard MNI space [20]. Compared to the conventional algorithm, the DARTEL approach can provide more precise spatial normalization to the template [21]. We performed a non-linear deformation on the normalized segmented images with the CAT12 toolbox as part of the modulation step. This modulation compares the absolute amounts of tissue corrected for individual differences in brain size [22]. All segmented, modulated, and normalized GM and WM images were smoothed using 8-mm full-width-half-maximum Gaussian smoothing. The CT was evaluated according to the projection-based thickness method [23] (see **Supplementary material 1**).

Diffusion data

Individual pre-processing. The diffusion-weighted data were skull-stripped using the Brain Extraction Tool implemented in FSLv6.0 (http://fsl.fmrib.ox.ac.uk/fsl/fslwiki/) and then corrected for distortions caused by eddy currents and movements. The diffusion tensor (DT) was estimated on a voxel-by-voxel basis using the DTIfit toolbox, part of the FMRIB Diffusion Toolbox within FSL, to obtain fractional anisotropy (FA), mean (MD), axial (AD), and radial (RD) diffusivities maps, the latter obtained by averaging L2 and L3 images. A bedpostX processing was done on eddy-current corrected images to allow probabilistic tractography analysis later.

Exploratory TBSS analysis. An exploratory tract-based spatial statistics (TBSS) was performed on the whole group. Individual FA images of all subjects were non-linearly registered to a standard fractional anisotropy template (http://fsl.fmrib.ox.ac.uk/fsl/fslwiki/FMRIB58_FA). We did not create a study-specific skeleton template, but we non-linearly reported each subject's fractional anisotropy map to the FMRIB58 skeleton (parameter –T in the tbss_3_postreg script). This was done to better segment our results with

the XTRACT atlas, as described later. The same operations were subsequently applied to the individual mean, axial, and radial diffusivity images using the previously calculated transformation. Voxelwise cross-subject statistics were then applied to these data.

TBSS Results segmentation. To understand which tracts the TBSS significant voxels belonged to and which tract percentage extent they covered, significant maps resulting from TBSS analysis were segmented according to the tracts defined in the XTRACT atlas. To do this, we first created a skeletonized version of each XTRACT's tract in the standard space by masking the FMRIB58 skeleton with each volume of the xtract-tract-atlases-maxprob5-1mm image. The number of voxels composing each skeletonized XTRACT atlas tracts was calculated. Then, we masked TBSS results with each of these skeletonized tracts, and we calculated the number of significant voxels belonging to each of these tracts and their coverage percentage (the number of voxels divided by the number of voxels composing each tract *100). Mean FA (and other metrics scores) values of the significant skeleton voxels within each subject tract were correlated to the SP score of interest to exclude any outlier subject. The CC region, not present in the XTRACT atlas, was obtained from the “Atlas of Human Brain Connections” (http://bcblab.com/BCB/Atlas_of_Human_Brain_Connections.html).

Tractography of tracts of interest. In those tracts where more than 10% of the voxels were significant, an automated XTRACT analysis, using its default settings, was performed in the native space of each subject. Mean tract values, averaging all the voxels belonging to each tract, were calculated. Individual mean values within CC were calculated in the FMRIB58 space considering all the 31704 voxels of such tract.

Resting-state functional connectivity analysis. A well-established analysis pipeline, tested on children [24,25] and adults [26–28] was run. Here, we first run a within-network functional connectivity (FC) analysis of DMN. Then, a seed-based FC analysis was run from those DMN clusters whose connectivity was modulated by AASP subscale scores. Since no correlations with any AASP scores emerged, details of this analysis were described elsewhere (see **Supplementary material**).

Statistical analysis. Regardless of the specific implementation of either FSL or SPM software, the same General Linear Model was tested, the four factors of each sensory profile set and subjects' age and gender were used as regressors. Contrasts evaluated each factor's positive and negative correlation, correcting for the two latter values.

Anatomical data. CT and VBM analysis were performed with the multiple regression model of SPM using default parameters. Moreover, the ROI values (WM, GM, and CT) previously calculated were exported, and their relationship with sensory profiles scores was analyzed in R software using either parametric or non-parametric partial correlations, correcting for either age and gender. We reported only those significant correlations ($p<0.05$) that had an R-value over 0.3.

DTI data. For TBSS group analysis, two general linear models were designed, each composed of the four regressors of each sensory profile set (SP1 and SP2) and both age and gender subject information. All

values were demeaned. Correlation between DTI metrics and SP parameters was carried out with non-parametric permutation tests (5000 permutations) and output maps were threshold-free cluster enhancement (TFCE) corrected using a significance threshold of $p<0.05$. Mean DTI metrics on individual tracts obtained through tractography (or on FMRIB58 space template in the CC case) were correlated with the SP scores using Pearson correlation analysis (after having verified their normality through the Shapiro-Wilk test).

Declarations

Funding

No external funding was received for this study.

Competing interests

The authors declare no competing interests.

Acknowledgements

This work was developed within the DINOGMI Department of Excellence of MIUR 2018-2022 (law 232, 2016) and the ANTARES joint lab among the Unit for Visually Impaired People (IIT), the DINOGMI Department and the IRCCS San Martino Hospital.

Data availability statement

The datasets used and/or analysed during the current study available from the corresponding author on reasonable request

Author contributions

A.E. conceived the study, A.E. and A.I. contributed to the study design, the enrollment of the subjects, the collection, analysis, and interpretation of the data, and to the writing of the manuscript. M.B.A., A.T., D.E., C.C., and B.P. contributed to the enrollment of the subjects and data collection. B.E.Y., G.S., M.G., and M.A. revised the manuscript for critical intellectual content design. All authors read and approved the final manuscript. All data generated or analyzed during this study are included in this published article.

References

1. Miller, L. J. & Schaaf, R. C. Sensory Processing Disorder. *Encycl. Infant Early Child. Dev.* **1**–**3**, 127–136 (2008).
2. Bowyer, P. & Cahill, S. *Pediatric Occupational Therapy Handbook: A Guide to Diagnoses and Evidence-Based Interventions*. *Sereal Untuk* (2018).

3. LA, H., A, K., ME, W. & L, A.-Z. The Importance of Sensory Processing in Mental Health: A Proposed Addition to the Research Domain Criteria (RDoC) and Suggestions for RDoC 2.0. *Front. Psychol.* **10**, (2019).
4. Serafini, G., Engel-Yeger, B., Vazquez, G. H., Pompili, M. & Amore, M. Sensory Processing Disorders are Associated with Duration of Current Episode and Severity of Side Effects. *Psychiatry Investig.* **14**, 51–57 (2017).
5. Engel-Yeger, B. *et al.* Sensory Hypersensitivity Predicts Reduced Sleeping Quality in Patients With Major Affective Disorders. *J. Psychiatr. Pract.* **23**, 11–24 (2017).
6. Engel-Yeger, B. *et al.* Sensory processing patterns, coping strategies, and quality of life among patients with unipolar and bipolar disorders. *Rev. Bras. Psiquiatr.* **38**, 207–215 (2016).
7. Dunn, W., Little, L., Dean, E., Robertson, S. & Evans, B. The State of the Science on Sensory Factors and Their Impact on Daily Life for Children: A Scoping Review. *OTJR (Thorofare. N. J).* **36**, 3S-26S (2016).
8. Shiotsu, D. *et al.* Elucidation of the relationship between sensory processing and white matter using diffusion tensor imaging tractography in young adults. *Sci. Rep.* **11**, 12088 (2021).
9. Yoshimura, S. *et al.* Gray matter volumes of early sensory regions are associated with individual differences in sensory processing. *Hum. Brain Mapp.* **38**, 6206 (2017).
10. Ohta, H. *et al.* White matter alterations in autism spectrum disorder and attention-deficit/hyperactivity disorder in relation to sensory profile. *Mol. Autism 2020 111* **11**, 1–13 (2020).
11. Owen, J. P. *et al.* Abnormal white matter microstructure in children with sensory processing disorders. *Neuroimage (Amst).* **2**, 844 (2013).
12. Dunn, W. The impact of sensory processing abilities on the daily lives of young children and their families: A conceptual model. *Infants Young Child.* (1997) doi:10.1097/00001163-199704000-00005.
13. Engel-Yeger, B. & Dunn, W. Exploring the relationship between affect and sensory processing patterns in adults. *Br. J. Occup. Ther.* (2011) doi:10.4276/030802211X13182481841868.
14. Serafini, G. *et al.* Extreme sensory processing patterns show a complex association with depression, and impulsivity, alexithymia, and hopelessness. *J. Affect. Disord.* **210**, 249–257 (2017).
15. Jerome, E. M. & Liss, M. Relationships between sensory processing style, adult attachment, and coping. (2004) doi:10.1016/j.paid.2004.08.016.
16. Ben-Avi, N., Almagor, M. & Engel-Yeger, B. Sensory Processing Difficulties and Interpersonal Relationships in Adults: An Exploratory Study. *Psychology* **03**, 70–77 (2012).
17. Engel-Yeger, B. *et al.* Extreme sensory processing patterns and their relation with clinical conditions among individuals with major affective disorders. *Psychiatry Res.* **236**, 112–118 (2016).
18. Rossi, A. *et al.* The reliability of the Mini-International Neuropsychiatric Interview–Italian version. *J. Clin. Psychopharmacol.* **24**, 561–563 (2004).
19. Ashburner, J. & Friston, K. J. Unified segmentation. *Neuroimage* **26**, 839–851 (2005).

20. Klein, A. *et al.* Evaluation of 14 nonlinear deformation algorithms applied to human brain MRI registration. *Neuroimage* **46**, 786–802 (2009).
21. Matsuda, H. *et al.* Automatic voxel-based morphometry of structural MRI by SPM8 plus diffeomorphic anatomic registration through exponentiated lie algebra improves the diagnosis of probable Alzheimer Disease. *AJNR. Am. J. Neuroradiol.* **33**, 1109–14 (2012).
22. Cousijn, J. *et al.* Grey matter alterations associated with cannabis use: results of a VBM study in heavy cannabis users and healthy controls. *Neuroimage* **59**, 3845–51 (2012).
23. Dahnke, R., Yotter, R. A. & Gaser, C. Cortical thickness and central surface estimation. *Neuroimage* **65**, 336–348 (2013).
24. Inuggi, A. *et al.* Brain functional connectivity changes in children that differ in impulsivity temperamental trait. *Front. Behav. Neurosci.* **8**, 156 (2014).
25. Sánchez-Pérez, N. *et al.* Computer-Based Cognitive Training Improves Brain Functional Connectivity in the Attentional Networks: A Study With Primary School-Aged Children. *Front. Behav. Neurosci.* **13**, 247 (2019).
26. Agosta, F. *et al.* Cortico-striatal-thalamic network functional connectivity in hemiparkinsonism. *Neurobiol. Aging* **35**, 2592–2602 (2014).
27. Imperiale, F. *et al.* Brain structural and functional signatures of impulsive–compulsive behaviours in Parkinson's disease. *Mol. Psychiatry* (2017) doi:10.1038/mp.2017.18.
28. Canu, E. *et al.* Breakdown of the affective-cognitive network in functional dystonia. *Hum. Brain Mapp.* **41**, 3059–3076 (2020).
29. Winston, G. P. *et al.* Diffusion tensor imaging tractography of the optic radiation for epilepsy surgical planning: A comparison of two methods. *Epilepsy Res.* **97**, 124 (2011).
30. Butler, P. D. *et al.* Early-Stage Visual Processing and Cortical Amplification Deficits in Schizophrenia. *Arch. Gen. Psychiatry* **62**, 495–504 (2005).
31. Schmahmann, J. D. & Pandya, D. N. Superior Longitudinal Fasciculus and Arcuate Fasciculus. *Fiber Pathways of the Brain* 393–408 (2009) doi:10.1093/ACPROF:OSO/9780195104233.003.0013.
32. Kamali, A., Flanders, A. E., Brody, J., Hunter, J. V. & Hasan, K. M. Tracing Superior Longitudinal Fasciculus Connectivity in the Human Brain using High Resolution Diffusion Tensor Tractography. *Brain Struct. Funct.* **219**, 269–281 (2014).
33. Barbeau, E. B., Descoteaux, M. & Petrides, M. Dissociating the white matter tracts connecting the temporo-parietal cortical region with frontal cortex using diffusion tractography. *Sci. Rep.* **10**, (2020).
34. Nakajima, R., Kinoshita, M., Shinohara, H. & Nakada, M. The superior longitudinal fascicle: reconsidering the fronto-parietal neural network based on anatomy and function. *Brain Imaging Behav. 2019 146* **14**, 2817–2830 (2019).
35. Denier, N. *et al.* Reduced tract length of the medial forebrain bundle and the anterior thalamic radiation in bipolar disorder with melancholic depression. *J. Affect. Disord.* **274**, 8–14 (2020).

36. Zhou, S.-Y. *et al.* Decreased volume and increased asymmetry of the anterior limb of the internal capsule in patients with schizophrenia. *Biol. Psychiatry* **54**, 427–436 (2003).
37. Mamah, D. *et al.* Anterior thalamic radiation integrity in schizophrenia: A diffusion-tensor imaging study. *Psychiatry Res. Neuroimaging* **183**, 144–150 (2010).
38. Coenen, V., Panksepp, J., Hurwitz, T., Urbach, H. & Mädler, B. Human medial forebrain bundle (MFB) and anterior thalamic radiation (ATR): imaging of two major subcortical pathways and the dynamic balance of opposite affects in understanding depression. *J. Neuropsychiatry Clin. Neurosci.* **24**, 223–236 (2012).
39. Brandes-Aitken, A. *et al.* White Matter Microstructure Associations of Cognitive and Visuomotor Control in Children: A Sensory Processing Perspective. *Front. Integr. Neurosci.* **12**, (2018).
40. Owens, M. M. *et al.* Neuroanatomical correlates of impulsive traits in children aged 9 to 10. *J. Abnorm. Psychol.* **129**, 831 (2020).
41. Tanaka-Arakawa, M. M. *et al.* Developmental Changes in the Corpus Callosum from Infancy to Early Adulthood: A Structural Magnetic Resonance Imaging Study. *PLoS One* **10**, (2015).
42. Fenlon, L. R. & Richards, L. J. Contralateral targeting of the corpus callosum in normal and pathological brain function. *Trends Neurosci.* **38**, 264–272 (2015).
43. De León Reyes, N. S., Bragg-Gonzalo, L. & Nieto, M. Development and plasticity of the corpus callosum. *Development* **147**, (2020).
44. Galinowski, A. *et al.* Resilience and corpus callosum microstructure in adolescence. *Psychol. Med.* **45**, 2285–2294 (2015).
45. Bubb, E. J., Metzler-Baddeley, C. & Aggleton, J. P. The cingulum bundle: Anatomy, function, and dysfunction. *Neurosci. Biobehav. Rev.* **92**, 104–127 (2018).
46. Bathelt, J., Johnson, A., Zhang, M. & Astle, D. E. The cingulum as a marker of individual differences in neurocognitive development. *Sci. Rep.* **9**, (2019).
47. Allman, J. M. *et al.* The anterior cingulate cortex. The evolution of an interface between emotion and cognition. *Ann. N. Y. Acad. Sci.* **935**, 107–117 (2001).
48. Holroyd, C. B. *et al.* Dorsal anterior cingulate cortex shows fMRI response to internal and external error signals. *Nat. Neurosci. 2004 75* **7**, 497–498 (2004).
49. Bettcher, B. M. *et al.* Neuroanatomical substrates of executive functions: Beyond prefrontal structures. *Neuropsychologia* **85**, 100–109 (2016).
50. Aminoff, E. M., Kveraga, K. & Bar, M. The role of the parahippocampal cortex in cognition. *Trends Cogn. Sci.* **17**, 379 (2013).
51. Bhattacharjee, S. *et al.* The Role of Primary Motor Cortex: More Than Movement Execution. *J. Mot. Behav.* **53**, 258–274 (2021).
52. Lafer-Sousa, R. & Conway, B. R. Parallel, multi-stage processing of colors, faces and shapes in macaque inferior temporal cortex. *Nat. Neurosci. 2013 1612* **16**, 1870–1878 (2013).

53. Lin, Y. H. *et al.* Anatomy and White Matter Connections of the Inferior Temporal Gyrus. *World Neurosurg.* **143**, e656–e666 (2020).
54. Palejwala, A. H. *et al.* Anatomy and White Matter Connections of the Lingual Gyrus and Cuneus. *World Neurosurg.* **151**, e426–e437 (2021).
55. Chen, Y. *et al.* Gray matter volumetric correlates of dimensional impulsivity traits in children: Sex differences and heritability. *Hum. Brain Mapp.* **43**, 2634–2652 (2022).
56. Briggs, R. G. *et al.* Anatomy and white matter connections of the inferior frontal gyrus. *Clin. Anat.* **32**, 546–556 (2019).
57. Rolls, E. T. Neural Computations Underlying Phenomenal Consciousness: A Higher Order Syntactic Thought Theory. *Front. Psychol.* **11**, (2020).
58. Swick, D., Ashley, V. & Turken, A. U. Left inferior frontal gyrus is critical for response inhibition. (2008) doi:10.1186/1471-2202-9-102.
59. Uddén, J. & Bahlmann, J. A rostro-caudal gradient of structured sequence processing in the left inferior frontal gyrus. *Philos. Trans. R. Soc. Lond. B. Biol. Sci.* **367**, 2023–2032 (2012).
60. Liakakis, G., Nickel, J. & Seitz, R. J. Diversity of the inferior frontal gyrus—A meta-analysis of neuroimaging studies. *Behav. Brain Res.* **225**, 341–347 (2011).
61. Reynaud, E., Navarro, J., Lesourd, M. & Osiurak, F. To Watch is to Work: a Review of NeuroImaging Data on Tool Use Observation Network. *Neuropsychol. Rev.* **29**, 484–497 (2019).
62. DiGuiseppi, J. & Tadi, P. Neuroanatomy, Postcentral Gyrus. *StatPearls* (2021).
63. Chen, X.-J., Liu, Y.-H., Xu, N.-L. & Sun, Y.-G. Multiplexed representation of itch and mechanical and thermal sensation in the primary somatosensory cortex. *J. Neurosci.* JN-RM-1445-21 (2021) doi:10.1523/JNEUROSCI.1445-21.2021.
64. Johns, P. Functional neuroanatomy. *Clin. Neurosci.* 27–47 (2014) doi:10.1016/B978-0-443-10321-6.00003-5.

Figures

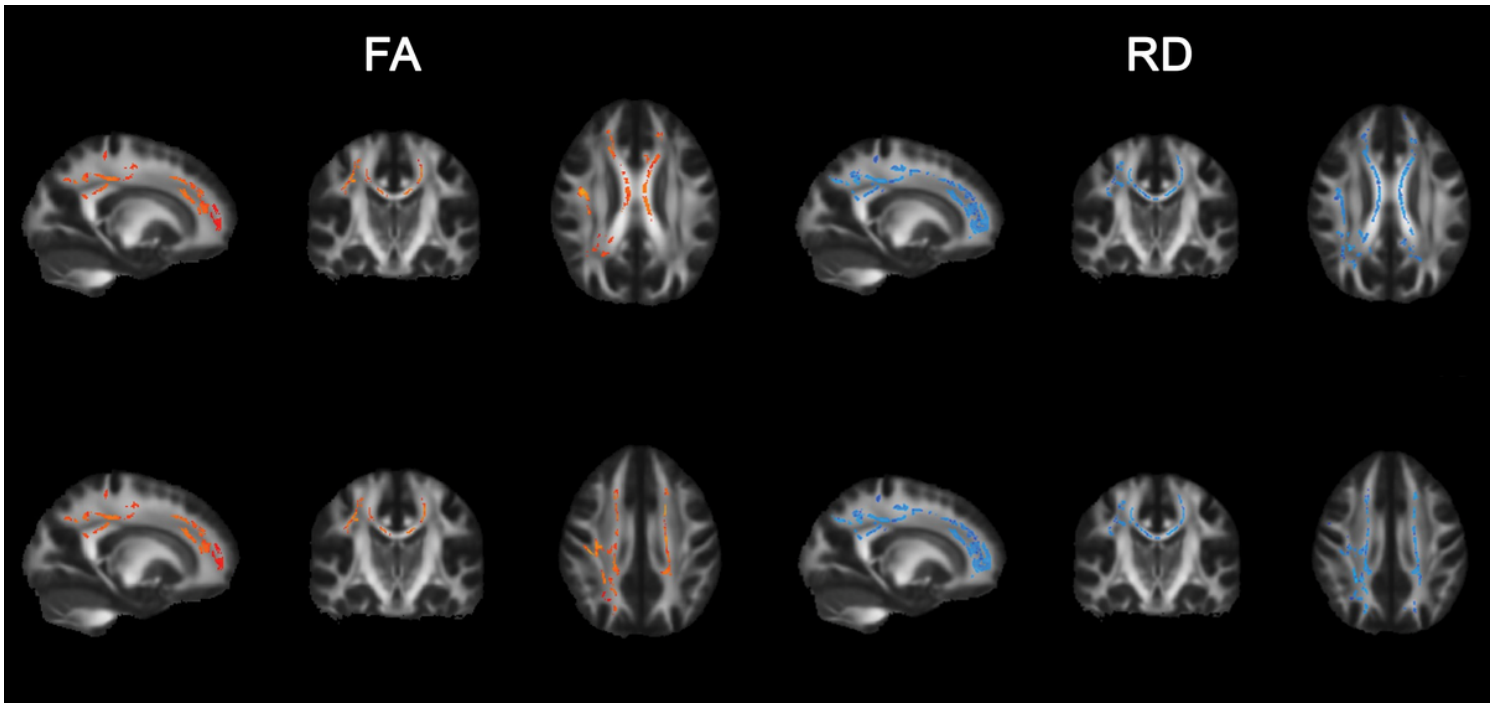

Figure 1

TBSS results. Positive (left) and negative (right) correlation between SP_STS and FA and RD.

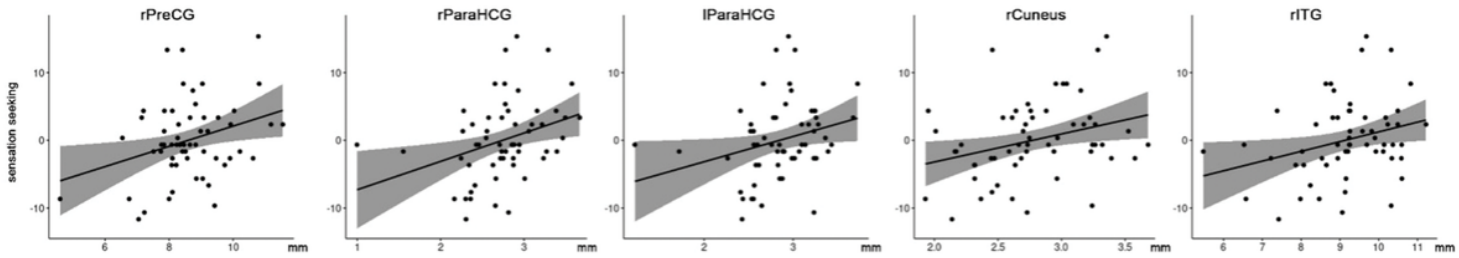

Figure 2

Correlations between sensation seeking and gray matter volumes in 5 ROI of the Neuromorphmetric atlas.

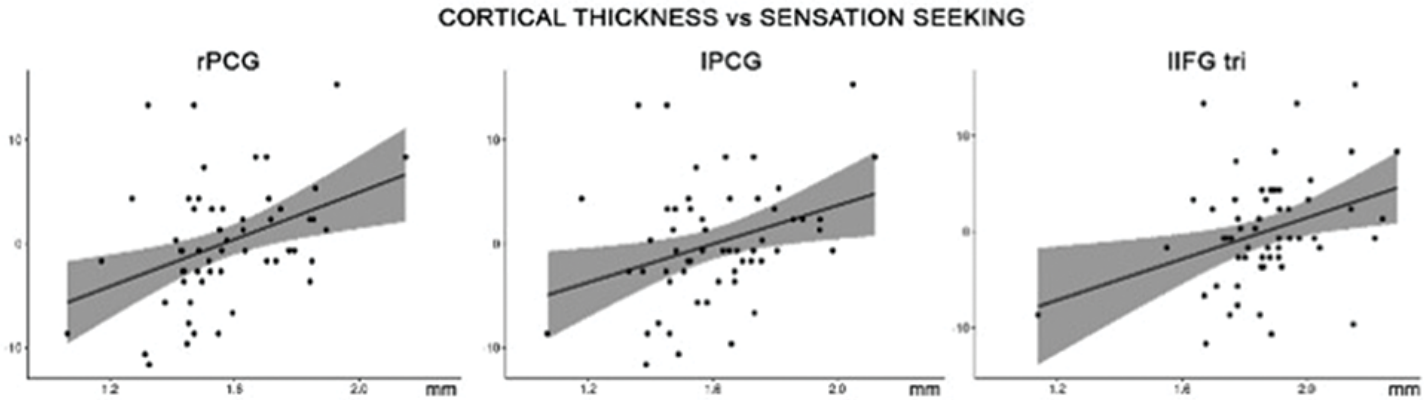

Figure 3

Correlations between sensation seeking and cortical thickness in three ROI of the a2000s atlas

Supplementary Files

This is a list of supplementary files associated with this preprint. Click to download.

- Supplementarymaterial.pdf